Eigen-Spectrum Estimation and Source Detection in a Massive Sensor Array Based on Quantum Assisted Hamiltonian Simulation Framework

Mostafizur Rahaman Laskar, *Student Member, IEEE*, Subhadeep Mondal, *Graduate Student Member, IEEE*, and Amit Kumar Dutta, *Member, IEEE*

***Abstract*— In this work, we propose quantum assisted eigenvalue estimation and target detection algorithms for a large sensor array via Hamiltonian simulation. Quantum algorithms provide complexity advantage of a certain class of problems on a quantum computer with fewer physical resources as compared to their classical counterparts. The proposed algorithms make use of the quantum phase estimation (QPE) as its core computing component. We have introduced an analytical quantum framework to map from classical to quantum in the context of target detection. Target detection involves an appropriate choice of threshold based on the probability of detection or false alarm. We exploited the massive sensor array structure and invoked the random matrix theory to propose an optimal threshold. It also takes into account the quantum measurement noise in the framework. Numerical simulations are performed to ascertain the efficacy of the proposed framework. The results suggest near term applications of the quantum algorithm for large-scale linear systems.**

***Index Terms*— Quantum signal processing, quantum eigenvalue estimation, quantum phase estimation, Hamiltonian simulation, array signal processing.**

I. Introduction

SENSOR arrays with multiple-input and multiple-output (MIMO) have become the forefront in modern signal processing and communication systems with a number of dedicated applications. They include beam-forming, precoding, source localization that improve the reliable detection and estimation of parameters of interest in a wireless system. The large arrays facilitate higher diversity and multiplexing gains, enhance channel estimation, and excellent efficiency in signal recovery [1], [2]. Few concurrent systems include the recent Terahertz (THz) communication [3], [4], robust source localization [5], and MIMO radar [6], where large number of antenna arrays have been used. As the sensor arrays are kept much higher than the number of parameters of sources, the underlying matrix of the system model seems to be sparse in nature [4]. We have considered a generalized sparse signal model of sensor arrays, while we use extended models to MIMO in the spatial domain and beam-space MIMO for practical interest. However, our objective of this work is limited to the quantum-based framework design for finding the eigen-spectrum of the said sparse matrix. This is because many modern applications require knowledge of the spectrum (eigenvalues) of the underlying system matrix. However, estimation of the eigenvalues with classical eigenvalue decomposition (EVD) incurs higher computational complexity of $\mathcal{O}(N^3)$ with an $N \times N$ matrix [7]. Quantum signal processing will come as a great help in determining the eigenvalues due to the parallelism inherited in quantum computation. Albeit, quantum inspired classical algorithms may achieve computational advantage for low rank system [8].

A. Recent Advances in Quantum Signal Processing

To provide much faster computation, quantum formalism comes with a few revolutionizing phenomena such as quantum parallelism, superposition and interference, quantum tunnelling, and entanglement [9]. Some of the potential applications include quantum communication (QC), quantum cryptography, quantum information theory (QIT) and others [10], [11]. However, most of the works in this area can be categorized into two major disciplines based on the quantum framework. One is the quantum search algorithm (QSA) [12], [13] and the other is the quantum simulation-based algorithms, such as Hamiltonian simulation [14] and quantum Fourier transform [15]. Based on QSA, a number of applications are proposed in the literature such as quantum assisted maximum likelihood algorithm, iterative quantum multi-user detector design [16], localization problem of mm-Wave communication [17], non-coherent multiple symbol detection [18], spatial division multiple access [19], channel estimation [20], non-orthogonal multiple access (NOMA) [21], and the sparse code multiple access detection [22]. There have been a few notable works conceived for the iterative quantum receiver with QSA [23], quantum Pareto optimization in network routing problems [24], and recently signal detection for MIMO with orthogonal frequency division multiplexing (MIMO-OFDM) systems [25]. Recent works also include quantum inspired classical algorithms [26], [27] and [8] for low rank

Manuscript received September 22, 2021; revised January 16, 2022; accepted April 6, 2022. Date of publication April 13, 2022; date of current version June 16, 2022. The associate editor coordinating the review of this article and approving it for publication was I. B. Djordjevic. *(Corresponding author: Amit Kumar Dutta.)*

The authors are with the G.S. Sanyal School of Telecommunications, Indian Institute of Technology Kharagpur, Kharagpur 721302, India (e-mail: m.rahaman93@gmail.com; braveknight701@gmail.com; amitdutta@gssst.iitkgp.ac.in).

Color versions of one or more figures in this article are available at https://doi.org/10.1109/TCOMM.2022.3167057.

Digital Object Identifier 10.1109/TCOMM.2022.3167057

0090-6778 © 2022 IEEE. Personal use is permitted, but republication/redistribution requires IEEE permission.
See https://www.ieee.org/publications/rights/index.html for more information.

Authorized licensed use limited to: ULAKBIM UASL - DOKUZ EYLUL UNIVERSITESI. Downloaded on October 28,2022 at 12:45:57 UTC from IEEE Xplore. Restrictions apply.

system, which attain computational speed-up. However, the quantum simulation-based detection and estimation problems remain an open-ended area to be researched.

B. Motivation of This Work

The motivation behind this work is to augment the power of quantum simulations to support the process of finding the eigenvalues of a massive matrix. This is the central problem for detecting objects using massive sensor arrays, where a covariance matrix is used. The inherent property of quantum parallelism is exploited in this computation. Unlike decomposing such matrix into its diagonal form via classical EVD method, quantum-Hamiltonian simulation can be used to prepare a unitary operator $\mathbf{U}$ using Hamiltonian-$\mathbf{S}$ as $\mathbf{U} = e^{-i\mathbf{S}t}$ with a proper quantum time-resolution (QTR) t (defined in Subsection B of Section-III), that facilitates the computation of the eigen-spectrum via the quantum phase estimation (QPE). If $\mathbf{S}$ is a d-sparse Hamiltonian, the simulation can be performed in $\mathcal{O}(\tau \log(\frac{\tau}{\epsilon})/\log\log(\frac{\tau}{\epsilon}))$, with $\tau = d^2||\mathbf{S}||_{max}t \geq 1$ and the overall permissible error being bounded by ϵ [28]. This is computationally much faster than the classical algorithms. This motivates us to reformulate the problem of estimation and detection of sources using quantum computation. We have shown applications of quantum eigenvalue estimation (QEE) for source identification and localization problems, whereby we propose quantum assisted detection and estimation algorithms for multiple sources. We have also discussed the effect of time-resolution and measurement uncertainty of the outcome of QPE on measurement bases, and the error model in the result and discussion part. Simulations are performed on both classical computers, as well as IBM quantum simulator [29] for the implementation of the algorithms.

C. Contributions

With the above background, our contributions in this paper are summarised as follows.

- A quantum framework with Hamiltonian simulation in a large sensor array is proposed, where object detection is performed. This proposal has several technical novelties in its fold.
  1) We propose a semi-quantum algorithm known as quantum assisted source detection algorithm (QA-SDA) for object detection in a massive sensor array with the Neyman-Pearson (NP) framework. In the first step, Hamiltonian simulation-based phase estimation is performed for computing the eigenvalues of a massive dimensional covariance matrix arising from the sensor array. This reduces the computational complexity, taking the advantage of quantum computing. In the second stage, an NP criteria is adopted, where the eigenvalues are compared with a threshold to detect the presence of objects.
  2) The threshold value is determined from a target probability of detection or probability of false alarm. We choose the former. However, no prior probability distribution of eigenvalue is assumed for threshold. In this work, we exploit the large dimension random matrix theory [30] to first determine the prior probability of this eigenvalue and then incorporate two random valued errors into it. The first one is a standard residual Gaussian noise error, and the other one is the quantum measurement noise. This quantum measurement noise is a discrete random variable, contrary to any Gaussian estimation error.
  3) A detailed analytical bound has been conceived for determining this threshold. We have also proposed a closed form bound with certain approximations.
- We have proposed a quantum-assisted multiple signal classification (QA-MUSIC) algorithm for angle of arrival (AoA) estimation in this multiple source localization problem frameworks. This is also a semi-quantum algorithm exploiting the Hamiltonian simulation-based phase estimation method.
- The quantum measurement noise is a drawback of every quantum system. However, properly determining this probability of error is conceived in a simple quantum signal processing application. In this work, we derive the exact probability of quantum measurement noise considering all the quantum building blocks and their effects.
- We have also done a computational complexity analysis for the proposed scheme and compared it with the one for a traditional system.
- Further, we have shown the circuit-level implementation of single-phase estimation on a real quantum computer provided by IBM, which shows attractive measurement outcome probability of the estimated outcome.

D. Mathematical Notations

Some mathematical notations and symbols used in this article are described below.
$|\psi\rangle \in \mathbf{C}^{n\times 1}$: A quantum state vector in column form.
$\rho = |\psi\rangle\langle\psi|$: Density matrix of pure state.
$\mathbf{C}, \mathbf{C^n}, \mathbf{C^{m\times n}}$: Set of complex number, vector, and matrices.
$||\mathbf{A}||_{\mathbf{p}}$,: p-norm of matrix A.
$\sigma_i(\mathbf{A})$: i^{th} eigenvalue of $\mathbf{A} \in \mathbf{C}^{N\times N}$ for $i \in (1, 2, \ldots, N)$.
$Tr(\mathbf{A})$: trace of matrix $\mathbf{A}$.
diag(σ_j): diagonal matrix with σ_j elements at j^{th} positions.
span$(v_1, v_2, \ldots, v_n)$: span defined by vectors $v_1, v_2, \ldots, v_n$ over the complex field $\mathbf{C}$.
dim$(\mathbf{S})$: dimension of the matrix $\mathbf{S}$.
x, $\mathbf{x}$, $\mathbf{X}$: scalar, vector and matrix quantity.
$\mathbf{C}^{n\times 1}$, $\mathbf{C}^{1\times n}$ column vector and row vector respectively.
$\mathbf{A}^\dagger, \mathbf{a}^\dagger$: complex conjugate transpose of the matrix "$\mathbf{A}$", and vector "$\mathbf{a}$", respectively.

II. System Model

We depict a system model having N sensor antennas and K-sources (objects) as shown in Fig. 1. We assume that it receives a complex signal vector $\mathbf{x} \in \mathbb{C}^{K\times 1}$ from K-sources, incident on a uniform linear array (ULA) of sensors with size N. The received data vector is represented by

$$\mathbf{s} = \boldsymbol{\Upsilon}^\dagger \mathbf{x} + \boldsymbol{\eta}, \tag{1}$$

Authorized licensed use limited to: ULAKBIM UASL - DOKUZ EYLUL UNIVERSITESI. Downloaded on October 28,2022 at 12:45:57 UTC from IEEE Xplore. Restrictions apply.

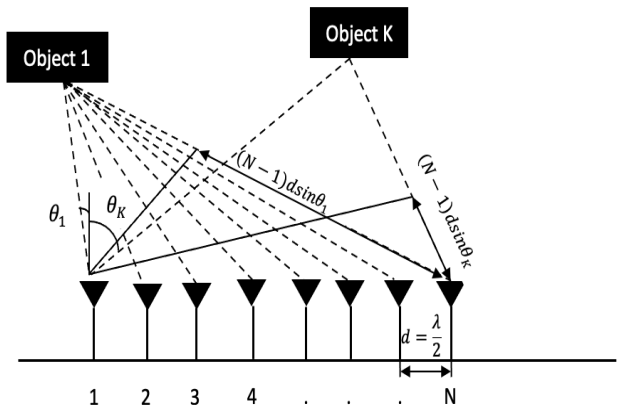

Fig. 1. A receiver front-end with linear uniform sensor array of size N, sensing incident rays from K objects.

where $\boldsymbol{\Upsilon} \in \mathbb{C}^{N\times K}$ represents the steering matrix, $\mathbf{s} \in \mathbb{C}^{N\times 1}$ denotes received vector. Also, $\boldsymbol{\eta} \in \mathbb{C}^{N\times 1}$ is assumed to be circularly symmetric, independent and identically distributed zero-mean additive white Gaussian noise (AWGN) vector. The steering matrix $\boldsymbol{\Upsilon}$ is represented as a sequence of K-steering vectors, each with dimension $N \times 1$, and is given by

$$\boldsymbol{\Upsilon} = [\mathbf{a}(\theta_1), \mathbf{a}(\theta_2), \ldots, \mathbf{a}(\theta_K)]^{\dagger}, \tag{2}$$

where the $\mathbf{a}_i \in \mathbb{C}^{N\times 1}$ for $i = 1, \ldots, N$ denotes the ith steering vector, and $\theta_1, \theta_2, \ldots, \theta_K$ represent the spatial directions of incoming signals at the receiver from K-sources.

In Fig. 1, the inclination angles of received signal are $\theta_1, \theta_2, \ldots, \theta_K$ with inter-element distance of $d = \lambda/2$, where λ is the wavelength of the transmitted signal. The sparsity aspect appears in the model, as we choose $N \gg K$ [4]. The covariance matrix $\mathbf{S} \in C^{N\times N}$ is estimated statistically from $\mathbf{s}$ as follows

$$\mathbf{S} = \mathbb{E}[\mathbf{s}\mathbf{s}^{\dagger}], \tag{3}$$

where $\mathbb{E}[.]$ denotes the expectation operator. In array signal processing, the matrix $\mathbf{S}$ holds certain structures such as normal matrix, Hermitian, Vandermonde, Toeplitz [31], or a Wishart Matrix, and sometimes sparse (for $N \gg K$). Often, we are interested to find the spectral estimate of $\mathbf{S}$ for several signal processing applications such as finding the model order, estimation of AoA of the signals, finding maximum power component, detection of the desired signal, and finding signal and noise subspace. However, we are limiting our work to detect the number of sources and estimate their positions via proposed quantum-inspired algorithms. In classical system, the spectrum of $\mathbf{S}$ is computed by EVD of $\mathbf{S}$ as

$$\mathbf{S} = \mathbf{Q}\boldsymbol{\Sigma}\mathbf{Q}^{\dagger} = \sum_{i=1}^{L} \sigma_i \mathbf{e}_i e_i^{\dagger}, \tag{4}$$

where $\mathbf{Q} \in \mathbb{C}^{N\times N}$ is a unitary matrix that contains the eigenvectors $(\mathbf{e}_1, \mathbf{e}_2, \ldots, \mathbf{e}_N)$, and the matrix $\boldsymbol{\Sigma} \in \mathbb{R}^{N\times N}$ is a diagonal matrix with ordered eigenvalues $(\sigma_1 \geq \sigma_2 \geq \cdots \geq \sigma_N)$ along its primary diagonal element. The covariance matrix can be written as follows

$$\mathbf{S} = \mathbf{S}_{xx} + \sigma_w^2 \mathbf{I}, \tag{5}$$

where the overall covariance matrix $\mathbf{S}$ comprises of two components: a signal-covariance matrix $\mathbf{S}_{xx}$ (which is low-rank for $K < N$), and $\sigma_w^2\mathbf{I}$ is the noise-covariance matrix (which regularizes the low-rank matrix $\mathbf{S}_{xx}$).

III. Background: Quantum Assisted Hamiltonian Simulation

A. Quantum Formalism

In this section, an introductory description of quantum computation is shown including state vector representation, quantum operation, some fundamental sub-routines, and measurement.

1) State and Basis: The basic computational element in a quantum computer is the qubit, which follows a set of quantum mechanical principles. A quantum state vector or simply 'state', $|\psi\rangle$ can be represented as the superposition of orthogonal unit vectors (basis) associated with probabilities as follows

$$|\psi\rangle = \alpha\,|0\rangle + \beta\,|1\rangle, \tag{6}$$

where, $|0\rangle$ and $|1\rangle$ are computational basis vectors, with associated probabilities $|\alpha|^2$ and $|\beta|^2$, which follow $|\alpha|^2+|\beta|^2 = 1$. Apart from computational basis, there are other basis, such as Fourier basis or sign basis, $|+\rangle$ and $|-\rangle$, which are related to computational basis as

$$|+\rangle = \frac{|0\rangle + |1\rangle}{\sqrt{2}}, \tag{7}$$

$$|-\rangle = \frac{|0\rangle - |1\rangle}{\sqrt{2}}. \tag{8}$$

However, computational basis states are predominantly adopted to represent a quantum framework compared to other basis states. With this basic framework description, a quantum system comprising of N computational basis states, i.e., $|0\rangle, |1\rangle, \ldots, |N-1\rangle$ with amplitudes $\alpha_0, \alpha_1, \ldots, \alpha_{N-1}$ is represented as follows

$$|\boldsymbol{\psi}\rangle = \alpha_0|0\rangle + \alpha_1|1\rangle + \ldots\ldots + \alpha_{N-1}|N-1\rangle, \tag{9}$$

with the condition stated as $\sum_{i=0}^{N-1} |\alpha_i|^2 = 1$.

2) Quantum Operations: A key phenomena in quantum mechanics is that the quantum states can possess a state transition by following the Schrodinger equation [32]. It indicates that the evolution of a quantum system can be illustrated by reversible operation. The reversible process can be realized using unitary transformation operator $\mathbf{U} \in \mathbb{C}^{N\times N}$ with the following condition $\mathbf{U}^{\dagger}\mathbf{U} = \mathbf{U}\mathbf{U}^{\dagger} = \mathbf{I}$.

B. Hamiltonian Simulation

The Hamiltonian simulation process helps to prepare the unitary operator $e^{-i\mathbf{S}t}$, for a given Hamiltonian $\mathbf{S}$ of size $N \times N$ in time t as efficiently as possible with suitable methods such as product formulas [14], truncated Taylor series [33], qubitization [34], quantum walk [35], and others. Mathematically, our objective is to simulate an approximate unitary operator given by,

$$\mathbf{U} \approx e^{-i\mathbf{S}t}. \tag{10}$$

Authorized licensed use limited to: ULAKBIM UASL - DOKUZ EYLUL UNIVERSITESI. Downloaded on October 28,2022 at 12:45:57 UTC from IEEE Xplore. Restrictions apply.

To implement this simulation with a permissible error bounded by ϵ, one of the well known choices is to represent the Hamiltonian $\mathbf{S} = \sum_{j=1}^{n} \mathbf{S}_j$. With this, the evolution operator can be approximated by a sequence of unitary operators given by $e^{-i\mathbf{S}_j t/n}$ [14], where n is the number of time-segments. The cost N_{exp} of this method is bounded by [14],

$$N_{exp} \leq n \times 5^{2k} \times (n\tau)^{1+\frac{1}{2k}} / \epsilon^{\frac{1}{2k}},$$

where, the term $\tau = ||\mathbf{S}||t$, and k denotes some integer. A further improvement is shown using a Taylor series approach [33], truncated at order K, and is given by

$$\mathbf{U}_n = e^{-i\mathbf{S}t/n} \approx \sum_{l=0}^{K} \frac{1}{l!} \left(-i\mathbf{S}t/n\right)^l. \tag{11}$$

For a d-sparse Hamiltonian $\mathbf{S}$, the complexity of the simulation for time t with permissible error bounded by ϵ is $\mathcal{O}\left(\tau \log(\frac{\tau}{\epsilon}) / \log\log(\frac{\tau}{\epsilon})\right)$, where the parameter $\tau = d^2 ||\mathbf{S}||_{max} t \geq 1$ [28]. For preparing the unitary $\mathbf{U}_N \in \mathcal{C}^{N\times N}$ via Hamiltonian simulation, the choice of time t is crucial. We define a time resolution called quantum time-resolution (QTR) below in the context of optimal Hamiltonian simulation.

1) Note on QTR: QTR is the minimum amount of time t required to prepare a unitary operator $\mathbf{U}_N \in \mathcal{C}^{N\times N}$ via Hamiltonian simulation of a Hermitian matrix $\mathbf{S} \in \mathbf{C}^{N\times N}$ where the error $||\mathbf{U}_N - e^{-i\mathbf{S}t}||$ is bounded by $\epsilon > 0$. An optimal QTR should be a very small amount of time t, such that the expected error in the simulation will converge asymptotically.

2) Assumptions for Hamiltonian Simulation: For a dense $N \times N$ Hamiltonian matrix $\mathbf{S}$, we may not find an efficient quantum simulation method. To augment the quantum speed-up for the proposed eigen-spectrum estimation, the following assumptions need to be taken care [36].

- The Hilbert space of $\mathbf{S}$ is a tensor product of many smaller sub-system components ($N = 2^m$ for a system of m-qubits).
- The matrix $\mathbf{S}$ is sparse with $\mathcal{O}(N)$ non-zero elements. In array signal processing, the sensor array size (N) should be enough large as compared to number of signals (K).
- The Hamiltonian has a complete description. In our case, the covariance matrix $\mathbf{S}$ is statistically estimated which is equivalent to a time-independent Hamiltonian.

As soon as we prepare the unitary operator $\mathbf{U}$ for the d-sparse Hermitian matrix $\mathbf{S}$, we can suitably proceed for a quantum evolution circuit to find out the eigenvalues of the matrix $\mathbf{S}$. One of the well-known subroutines that helps us find the spectrum of $\mathbf{S}$ is the QPE circuit, which is discussed next.

C. Quantum Phase Estimation

QPE includes a family of algorithms [37], [38] that estimate one of many phases σ_j of the unitary operator $\mathbf{U}$. We can write it as

$$\begin{aligned} \mathbf{U}\left|\psi\right\rangle_i &= \tilde{\sigma}_i \left|\psi\right\rangle_i \\ &= e^{i2\pi\sigma_i} \left|\psi\right\rangle_i, \end{aligned} \tag{12}$$

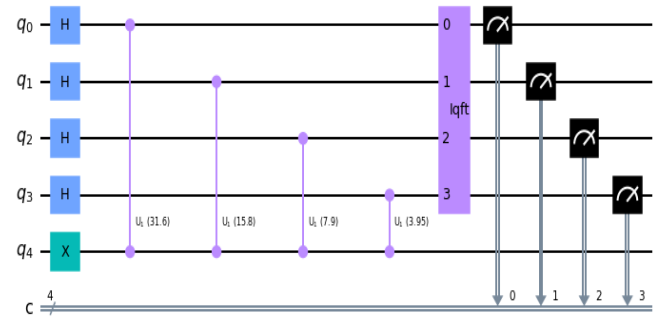

Fig. 2. Circuit of QPE (Implemented on IBM Quantum simulator with Qiskit Package) with 5 quantum registers($q's$), and 4 classical registers (c); U_1 are controlled rotation gates, and iqft represents the inverse quantum Fourier transform circuit; H denotes the Hadamard gate.

where, the $\left|\psi\right\rangle_i$ is an eigenstate of $\mathbf{U}$ and the corresponding eigenvalue is $\tilde{\sigma}_i$. The eigenvalue estimation for $\mathbf{S}$ is now mapped to phase estimation σ_i for the unitary operator $\mathbf{U} = e^{-i\mathbf{S}t}$.

Fig. 2 shows a shorter version of circuit of QPE simulated on IBM QISKIT quantum simulator [29] with four ancillary qubits represented by quantum registers q_0, q_1, q_2, q_3. and x contains the ith eigenstate $\left|\psi\right\rangle_i$ stored in the quantum-register q_4. Here, c represents classical registers where the measurement outcome will be stored. The successful implementation of QPE requires that the unitary $\mathbf{U}$ is conditioned on the state of the ancillary qubits in a controlled fashion given by

$$\tilde{\mathbf{U}} = \left|0\right\rangle\left\langle 0\right| \otimes \mathbf{I} + \left|1\right\rangle\left\langle 1\right| \otimes \mathbf{U}, \tag{13}$$

where, $\mathbf{I}$, denotes identity operator, and $\left|0\right\rangle$, $\left|1\right\rangle$ represent computational basis states of ancillary qubits $q's$. The superposition states of the $q's$ are generated by Hadamard gates H. One of the challenging tasks is to prepare the starting state, i.e the eigenstate of $\mathbf{U}$ in (12). In the IBM QISKIT platform, one may easily obtain the estimated phase of $\mathbf{U}$ on a measurement basis, where the probability is maximum, and precision of the estimated phase is obtained by the number of qubits that represent the basis in the binary numbers. Once we obtain the phases of the eigenvalues of $\mathbf{U}$, it readily produces the eigenvalues $\sigma_1, \ldots, \sigma_N$ of $\mathbf{S}$ with normalization.

IV. Proposed Quantum Algorithms in Source Detection and Localization

Source localization for sparse array system is of great interest [39], [40]. In this section, we propose two quantum assisted algorithms for a sparse-array system. The first one is on spectral detection, i.e the number of sources/user detection, and the second one is on localization problem, i.e the AoA estimation.

A. Proposed Quantum Assisted Source Detection Algorithm (QA-SDA)

Detection of the signal subspace dimension helps to provide the model order of many high-resolution parametric estimators [41]. We are interested to find the number of sources (K)

Authorized licensed use limited to: ULAKBIM UASL - DOKUZ EYLUL UNIVERSITESI. Downloaded on October 28,2022 at 12:45:57 UTC from IEEE Xplore. Restrictions apply.

present in an environment that determines the signal subspace dimension. For K number of sources and N sensor arrays, the covariance matrix $\mathbf{S} \in \mathbb{C}^{N\times N}$ can be approximated to a sparse-matrix with rank $K \ll N$. Here, the parameter K is unknown which needs to be estimated.

1) The Source Detection Problem: We propose a quantum assisted source detection algorithm (QA-SDA) to find the number of unknown sources K. This is a semi-quantum detection framework, where the eigenvalues are obtained by quantum Hamilton simulation, and the detection of signal-subspace dimension (K) is performed as a classical computation. We assume a maximum limit of K as K_{max}.

In determining the number of sources, it is required to estimate the non-zero eigenvalues of the Hermitian matrix $\mathbf{S}$ having a rank K. QEE estimates these eigenvalues. Thereafter, a classical NP detection method is used. Due to noise, the estimation of the eigenvalue will never be non-zero, where the target is absent. Hence, a threshold is used to determine if an eigenvalue exists or not. This leads to a hypothesis testing scheme as stated below,

$$\mathcal{H}_0 : x = \sigma_i < \sigma_{th}, \tag{14}$$

$$\mathcal{H}_1 : x = \sigma_i \geq \sigma_{th}. \tag{15}$$

Here, each eigenvalue σ_i obtained from QEE is stored in a classical register. A classical oracle compares each σ_i to a specified threshold σ_{th}. Due to the presence of residual zero-mean Gaussian noise w_e and the quantum measurement noise w_q, the σ_i can be represented as

$$\sigma_i = \tilde{\sigma}_i + w_q + w_\epsilon + w_e, \tag{16}$$

where $\tilde{\sigma}_i$ is the actual eigenvalue. Let us assume that the variance of w_e is σ_e^2, while w_q is a discrete valued measurement noise having mean zero and variance σ_q^2. Further the Quantum evolution uncertainty in preparation of $\mathbf{U}_N$ via Hamiltonian simulation is modelled as additive noise component w_ϵ which has zero mean and variance of ϵ^2 (Derivation is in Subsection-A of Section-V). The total residual noise variance is $\sigma_w^2 = \sigma_e^2 + \sigma_q^2 + \epsilon^2$. The σ_e^2 can be obtained from Cramer Rao lower bound (CRLB) or Bayesian-CRLB (BCRLB) based on estimation technique. The noise w_q arises due to quantum probabilistic measurement.

The null-hypothesis ($\mathcal{H}_0$) states that any eigenvalue below the threshold can be considered to be zero. The $\mathcal{H}_1$ hypothesis favours the acceptance of eigenvalues above the threshold. The number of non-zero eigenvalues that favours $\mathcal{H}_1$ is referred to as K. To find a suitable threshold, one needs to consider the likelihood function of x given by

$$\int_{\sigma_{th}}^{\infty} P(x|\tilde{\sigma}_i)P(\tilde{\sigma}_i)d\tilde{\sigma}_i = \gamma. \tag{17}$$

Here, γ is the probability of detection for the designed experiment. Let us define a general constant as $C_k = \frac{1}{2}\left(\frac{-1}{2}\right)\ldots\left(\frac{3-2k}{2}\right)$.

Theorem 1: For a large dimension receiving array size, the threshold σ_{th} in the hypothesis is related as a non-linear function of the probability of detection γ as follows

$$\gamma \geq 2\pi - 4\sin^{-1}\sqrt{\frac{\sigma_{th}}{4}} - 2\sin\left(2\sin^{-1}\sqrt{\frac{\sigma_{th}}{4}}\right) - \int_{\sigma_{th}}^{4}\left[\frac{4}{\sqrt{\sigma}}\sum_{k=0}^{\infty}\frac{C_k}{k!}(-1)^k\left(\frac{\sigma}{4}\right)^k\right] exp\left(\frac{-1}{2}\frac{\sigma^2}{\sigma_w^2}\right)d\sigma, \tag{18}$$

Proof: From (17), we may expand γ considering $p(x|\sigma_i)$ as Gaussian distributed with mean σ and variance σ_w^2, as follows

$$\gamma = \int_0^{\infty}\int_{\sigma_{th}}^{4}\left(\frac{1}{2\pi\sigma_w^2}\right)^{\frac{1}{2}}\exp\left(-\frac{1}{2\sigma_w^2}(x-\sigma)^2\right)p(\sigma)dxd\sigma. \tag{19}$$

Following large-dimension matrix theory [30], the distribution of eigenvalues of the matrix $\mathbf{S}$ is given by

$$p(\sigma) = \left(1-\frac{1}{\sigma}\right)^+\delta(\sigma)+\frac{1}{2\pi c\sigma}\sqrt{(\sigma-a)^+(b-\sigma)^+} \tag{20}$$

Here, x^+ is defined as $x^+ = x$ for $x > 0$. Note that, the parameter $c = 1$ (it is the ratio of transmitting and receiving antenna size, taken to be 1 here), $a = (1-\sqrt{c})^2 = 0$, and $b = (1+\sqrt{c})^2 = 4$. Considering $p(\sigma)$ as defined in (20), the expression for γ in (19) becomes

$$\gamma = \frac{1}{\sqrt{2\pi}\sigma_w}\int_0^{\infty}\int_{\sigma_{th}}^{4}\exp\left(-\frac{(x-\sigma)^2}{2\sigma_w^2}\right)\left(\frac{4-\sigma}{\sigma}\right)^{\frac{1}{2}}dxd\sigma. \tag{21}$$

Further, we solve (21) as follows

$$\begin{aligned}\gamma &= \int_0^{\infty}\left(\frac{1}{\sigma_w\sqrt{2\pi}}\right)\int_{\sigma_{th}}^{4}\exp\left(-\frac{1}{2}\left(\frac{x-\sigma}{\sigma_w}\right)^2\right)\left(\frac{4-\sigma}{\sigma}\right)^{\frac{1}{2}}dxd\sigma \\ &= \frac{1}{\sqrt{2\pi}\sigma_w}\int_{\sigma_{th}}^{4}\left[\int_{\frac{-\sigma}{\sigma_w}}^{\infty}\exp\left(\frac{-y^2}{2}\right)\sigma_w dy\right]\left(\frac{4-\sigma}{\sigma}\right)^{\frac{1}{2}}d\sigma.\end{aligned} \tag{22}$$

Note that, we have considered $y = \frac{x-\sigma}{\sigma_w}$, and adjusted the limit of the integral accordingly. Hence, the we obtain the expression of $Q(.)$ function from the above integral and the reduced form is given by

$$\gamma = \int_{\sigma_{th}}^{4}\left[1-Q\left(\frac{\sigma}{\sigma_w}\right)\right]\left(\frac{4-\sigma}{\sigma}\right)^{\frac{1}{2}}d\sigma. \tag{23}$$

Introducing the bound for $Q(y) \leq exp(\frac{-y^2}{2})$ and $y > 0$ in the above expression, the integral becomes

$$\begin{aligned}\gamma &\geq \int_{\sigma_{th}}^{4}\left[1-\exp\left(\frac{-\sigma^2}{2\sigma_w^2}\right)\right]\left(\frac{4-\sigma}{\sigma}\right)^{\frac{1}{2}}d\sigma \\ &= \int_{\sigma_{th}}^{4}\left(\frac{4-\sigma}{\sigma}\right)^{\frac{1}{2}}d\sigma - \int_{\sigma_{th}}^{4}exp\left(\frac{-\sigma^2}{2\sigma_w^2}\right)\left(\frac{4-\sigma}{\sigma}\right)^{\frac{1}{2}}d\sigma.\end{aligned} \tag{24}$$

Authorized licensed use limited to: ULAKBIM UASL - DOKUZ EYLUL UNIVERSITESI. Downloaded on October 28,2022 at 12:45:57 UTC from IEEE Xplore. Restrictions apply.

In the expression (24) of γ, let us consider that

$$I_1 \triangleq \int_{\sigma_{th}}^{4} \left(\frac{4-\sigma}{\sigma}\right)^{\frac{1}{2}} d\sigma. \tag{25}$$

In order to solve the integration, further we have considered that $\sigma = 4\sin^2\phi$ and adjusted the limit for change of variable from σ to ϕ, given as follows

$$\begin{aligned} I_1 &= \int_{\phi_l}^{\phi_u} \left(\sqrt{\frac{1-\sin^2\phi}{\sin^2\phi}}\right) 8\sin\phi\cos\phi d\phi \\ &= 2\pi - 4\sin^{-1}\sqrt{\frac{\sigma_{th}}{4}} - 2\sin\left(2\sin^{-1}\sqrt{\frac{\sigma_{th}}{4}}\right). \end{aligned} \tag{26}$$

Here, the limit of integral are $\phi_u = \pi/2$, and $\phi_l = \sin^{-1}\sqrt{\frac{\sigma_{th}}{4}}$. Hence, adopting (26) in the expression (24), the γ becomes

$$\gamma \geq I_1 - \int_{\sigma_{th}}^{4} exp\left(\frac{-1}{2}\frac{\sigma^2}{\sigma_w^2}\right)\left(\frac{4-\sigma}{\sigma}\right)^{\frac{1}{2}} d\sigma. \tag{27}$$

Let us consider the integral equation of (27) as

$$\begin{aligned} I_2 &\triangleq \int_{\sigma_{th}}^{4} exp\left(\frac{-1}{2}\frac{\sigma^2}{\sigma_w^2}\right)\left(\frac{4-\sigma}{\sigma}\right)^{\frac{1}{2}} d\sigma \\ &= \int_{\sigma_{th}}^{4} \left[\frac{4}{\sigma}\left(1-\frac{\sigma}{4}\right)\right]^{1/2} exp\left(\frac{-\sigma^2}{2\sigma_w^2}\right) d\sigma \\ &= \int_{\sigma_{th}}^{4} \left[\frac{2}{\sqrt{\sigma}}\sum_{k=0}^{\infty}\frac{C_k}{k!}(-1)^k\left(\frac{\sigma}{4}\right)^k\right] exp\left(\frac{-\sigma^2}{2\sigma_w^2}\right) d\sigma. \end{aligned} \tag{28}$$

The closed-form solution to (28) may not be achieved as the integral does not possess elementary function(s) of finite order. Hence, the expression for σ_{th} with γ is given by (29), as shown at the bottom of the page. ■

Lemma 1: With first order approximation, the false alarm probability γ of the hypothesis can be represented as in (30)*, as shown at the bottom of the page.*

Proof: In order to get an approximate solution for σ_{th} related to γ (29), we use Taylor series approximation of the term $\left(\frac{4-\sigma}{\sigma}\right)^{\frac{1}{2}}$ with the first two terms and ignoring rest as follows

$$\left(\frac{4-\sigma}{\sigma}\right)^{\frac{1}{2}} \approx \frac{2}{\sqrt{\sigma}}\left(1-\frac{\sigma}{8}\right). \tag{31}$$

Then, we obtain further as follows

$$I_2 = \int_{\sigma_{th}}^{4} \left(\frac{2}{\sqrt{\sigma}} - \frac{\sqrt{\sigma}}{4}\right) exp\left(\frac{-1}{2}\frac{\sigma^2}{\sigma_w^2}\right) d\sigma. \tag{32}$$

To solve the above integral by parts, we consider $u = \left(\frac{2}{\sqrt{\sigma}} - \frac{\sqrt{\sigma}}{4}\right)$, and $v = exp\left(\frac{-1}{2}\frac{\sigma^2}{\sigma_w^2}\right)$. Hence, (32) becomes

$$I_2 = \left[u\int v d\sigma\right]_{\sigma_{th}}^{4} - \left[\int u'\left(\int v d\sigma\right) d\sigma\right]_{\sigma_{th}}^{4}. \tag{33}$$

where u' is the derivative of u which can be computed to be $u' = -\left[\frac{1}{\sigma^{3/2}} + \frac{1}{8\sqrt{\sigma}}\right]$. Now, we need to compute the integral $\int_{\sigma_{th}}^{4} v d\sigma$. As this integral cannot be computed as an elementary function, we consider the following (with expanded σ)

$$I_3 = \int v d\sigma = \int exp\left(\frac{-\sigma^2}{2\sigma_w^2}\right) d\sigma. \tag{34}$$

We take Taylor series approximation of the function $f(\sigma) = exp\left(\frac{-\sigma^2}{2\sigma_w^2}\right)$ about the point $\sigma = 0$, given as

$$f(\sigma) \approx f(0) + \sigma f'(0) + \mathcal{O}(l)^2, \tag{35}$$

$\mathcal{O}(l)^2$ is the approximation-residue with step length l. Further, computing the values of the terms, we can see $f(0) = 1$ and higher terms are zero. Hence, we obtain the first order approximation of I_3 as

$$\begin{aligned} I_3 &= \int f(0) d\sigma \quad (36) \\ &= \sigma. \quad (37) \end{aligned}$$

Now, I_2 can be written as

$$\begin{aligned} I_2 &= \left[u\ I_3 - \int u' I_3 d\sigma\right]_{\sigma_{th}}^{4} \\ &= \left[\left(\frac{2}{\sqrt{\sigma}} - \frac{\sqrt{\sigma}}{4}\right)\sigma + \int\left[\frac{1}{\sigma^{3/2}} + \frac{1}{8\sqrt{\sigma}}\right] I_3 d\sigma\right]_{\sigma_{th}}^{4} \\ &= \left[\left(\frac{2}{\sqrt{\sigma}} - \frac{\sqrt{\sigma}}{4}\right)\sigma\right]_{\sigma_{th}}^{4} + \left[\int\left[\frac{1}{\sigma^{3/2}} + \frac{1}{8\sqrt{\sigma}}\right] I_3 d\sigma\right]_{\sigma_{th}}^{4} \\ &= 2\sigma_{th}^{1/2} - \frac{1}{4}\sigma_{th}^{3/2} + I_4 \end{aligned} \tag{38}$$

where, the I_4 is computed as follows,

$$\begin{aligned} I_4 &= \left[\int\left[\frac{1}{\sigma^{3/2}} + \frac{1}{8\sqrt{\sigma}}\right]\sigma d\sigma\right]_{\sigma_{th}}^{4} \\ &= 2\sigma_{th}^{1/2} + \frac{1}{12}\sigma_{th}^{3/2} \end{aligned} \tag{39}$$

Hence, we get $I_2 = 4\sigma_{th}^{1/2} - \frac{1}{6}\sigma_{th}^{3/2}$. With (37), (38) and (39), the expression for $\gamma \geq I_1 - I_2$ in (27) becomes (30). ■

$$\gamma \geq 2\pi - 4\sin^{-1}\sqrt{\frac{\sigma_{th}}{4}} - 2\sin\left(2\sin^{-1}\sqrt{\frac{\sigma_{th}}{4}}\right) - \int_{\sigma_{th}}^{4}\left[\frac{2}{\sqrt{\sigma}}\sum_{k=0}^{n}\binom{n}{k}(-1)^k\left(\frac{\sigma}{4}\right)^k\right] exp\left(\frac{-1}{2}\frac{\sigma^2}{\sigma_w^2}\right) d\sigma. \tag{29}$$

$$\gamma \approx 2\pi - 4\sin^{-1}\sqrt{\frac{\sigma_{th}}{4}} - 2\sin\left(2\sin^{-1}\sqrt{\frac{\sigma_{th}}{4}}\right) - 4\sigma_{th}^{1/2} - \frac{1}{6}\sigma_{th}^{3/2}. \tag{30}$$

Authorized licensed use limited to: ULAKBIM UASL - DOKUZ EYLUL UNIVERSITESI. Downloaded on October 28,2022 at 12:45:57 UTC from IEEE Xplore. Restrictions apply.

The σ_{th} can be obtained by solving the below optimization problem using line search method as follows

$$\underset{\sigma_{th}}{\arg\min} \quad [\gamma - \Gamma(\sigma_{th})], \tag{40}$$

where, $\Gamma(\sigma_{th})$ is the right hand side part of (30). The overall QA-SDA algorithm is summarized in Algorithm-1.

Algorithm 1 Proposed QA-SDA

- **Input:** $\mathbf{s} \leftarrow \mathbf{0}_{N\times 1}$, $\mathbf{S} \leftarrow \mathbf{0}_{N\times N}$, $\boldsymbol{\Upsilon} \leftarrow \mathbf{0}_{N\times K}$, $t \leftarrow 0$, $R_1 \leftarrow 0$, $R \leftarrow 0$ N, K_{max}, σ_{th}, σ_e, σ_w, ϵ, $|\psi\rangle$, L, κ
- **Output:** K

  For $n = 1 : L$, **do:**
  $\mathbf{s}(n) \leftarrow \boldsymbol{\Upsilon}^{\dagger}\mathbf{x}(n) + \boldsymbol{\eta}(n)$;
  $\mathbf{S} \leftarrow \mathbb{E}[\mathbf{s}\mathbf{s}^{\dagger}]$ (Co-variance matrix)
  End For
- **Step-1: Hamiltonian Simulation**

  for $j = 1 : m$, **do:**
  $t \leftarrow 1/m$;
  $U \leftarrow exp(-i\sum_j U_j t)$ (Exact)
  for $l = 1 : m$, **do:**
  $\tilde{U} \leftarrow \sum_{l=0}^{\kappa} \frac{1}{l!m^l}(-i\sum_j U_j)^l$ (Approximation)
  while $(t > 0)$, **do:**
  If $(||U - \tilde{U}|| < \epsilon)$ (With precision ϵ)
  break;
  End If
  End For
  End For
- **Step-2: QPE**

  For $n = 1 : N$, **do:**
  $\phi_0 \leftarrow |0\rangle^{\otimes n}|\psi\rangle$ (Initialization);
  $\tilde{\psi}_1 \leftarrow \frac{1}{2^{n/2}}(|0\rangle + |1\rangle)^{\otimes n}|\psi\rangle$ (Superposition on ϕ_0)
  For $l = 1 : N$, **do:**
  $\tilde{\psi}_2 \leftarrow \frac{1}{2^{n/2}}\sum_{l=0}^{2^n-1} exp(2\pi i\theta l)|l\rangle \otimes |\psi\rangle$ (Successive U-rotations on $\tilde{\psi}_1$)
  For $h = 1 : N$, **do:**
  $\tilde{\psi}_3 \leftarrow \frac{1}{2^n}\sum_{h=0}^{2^n-1}\sum_{l=0}^{2^n-1} exp(\frac{2\pi ik}{2^n}(h - 2^n\theta))|h\rangle \otimes |\psi\rangle$ (IQFT of $\tilde{\psi}_2$ on register $|h\rangle$)
  End For
  End For
  End For
- **Step-3: Quantum Detection**

  For $i = 1 : K_{max}$, **do:**
  If $\sigma_i < \sigma_{th}$, **do:**
  $R1 = 0$
  Else do:
  $R1 = 1$
  End If
  $R \leftarrow$ get count $(R1 = 1)$; $K \leftarrow R$
  End For

2) Notes on QA-SDA: In Algorithm-1, the pseudo-code of QA-SDA algorithm is presented. The input variables, $\mathbf{s}, \mathbf{S}, \boldsymbol{\Upsilon}, \mathbf{N}, K_{max}, \sigma_{th}, \sigma_e, \sigma_w, L$ are defined in text; R_1, R, κ represent local variables, $|\psi\rangle$ denotes quantum eigenstate, and ϵ is the precision for Hamiltonian simulation. The output of QA-SDA is the number of sources K. Given the uniform linear array, we take the compute of the covariance matrix S based on the noisy observed signal $\mathbf{s}$. For QA-SDA, there are three major steps: (i) Hamiltonian simulation, (ii) Quantum phase estimation (QPE) with inverse quantum Fourier transform (IQFT), and (iii) threshold comparison at Quantum oracle. These are described as follows.

- **Step-**1 describes the Hamiltonian simulation of the covariance matrix $\mathbf{S}$. It takes a uniform sampling of the estimated covariance matrix following (10) with a series of truncated unitaries $\mathbf{U}_j$ given by (11). The iteration continues till it satisfies the condition of the desired accuracy, with given precision ϵ.
- In **step-**2, the QPE is shown. Here, n-length qubit is denoted with tensor representation. Hadamard operations are performed for the superposition of the ancillary qubits. U-gates are applied on the Hadamard output to control $|1\rangle$-bases for phase rotation. It is finally followed by the IQFT circuit on the auxiliary resisters $|h\rangle$. The measurement is performed at the output of the IQFT circuit on the computational basis to detect the phase changes of the qubits acted on the quantum eigenstates via the QPE circuit, from which eigenvalues can be obtained.
- As the estimated eigenvalues via QPE is not sorted, we execute **step-**3 for the comparison. The detection threshold is assumed to be σ_{th} and stored in quantum oracle. Every eigenvalues $(\sigma_i's)$ are compared with the σ_{th} at oracle. In quantum random access memory (QRAM), the oracle helps to count the number of eigenvalues greater than the threshold, which represents the detected number of sources, K.

B. Proposed Quantum Assisted MUSIC (QA-MUSIC) Algorithm for AoA Estimation

We propose the quantum assisted AoA estimation problem of multiple sources in a massive sensor array. Classical super-resolution AoA algorithms exploit the eigenvalues of $\mathbf{S}$ via eigenvalue decomposition (EVD) [42] for the localization of multiple signal-sources. However, the computational costs for EVD is extremely high for large arrays. We seek to embed the QPE-based quantum framework for the super-resolution AoA estimation problem. The proposed algorithm is called quantum assisted multiple signal classification (QA-MUSIC) as described in Algorithm-2.

1) Notes on QA-MUSIC: In the proposed QA-MUSIC case (Algorithm-2), we have four major steps: (i) Estimation of covariance matrix (ii) Hamiltonian simulation, (iii) QPE with IQFT, and (iv) spectrum estimation. Step (i) to (iii) are similar to QA-SDA as described earlier. At first, we perform Hamiltonian simulation (10) for preparing the unitary evolution operator $\mathbf{U}$ from the sparse-covariance matrix $\mathbf{S}$ with a sufficiently small QTR t. The array size is represented by N which is considered to be large. As QA-MUSIC is a parametric estimator, the model order of K, which determines the signal subspace dimension needs to be provided from QA-SDA. If K is unknown, K_{max} is provided. For the QPE, one needs to prepare the eigenstates $(|\psi\rangle = [|\psi\rangle_1, |\psi\rangle_2, \ldots, |\psi\rangle_N])$ quantum-mechanically that satisfies $\mathbf{U}|\psi\rangle_i = e^{i2\pi\sigma_i}|\psi\rangle_i$ (12). We perform single phase estimation on quantum computer, whereas for the large-dimensions of $\mathbf{S}$ and multiple eigenvalues, QPE is computed classically due to constrained-resources. In the second phase of the algorithm, we perform similar spectrum-based AoA estimation for multiple sources

Authorized licensed use limited to: ULAKBIM UASL - DOKUZ EYLUL UNIVERSITESI. Downloaded on October 28,2022 at 12:45:57 UTC from IEEE Xplore. Restrictions apply.

Algorithm 2 Proposed QA-MUSIC

- **Input:** $\mathbf{s} \leftarrow \mathbf{0}_{N\times 1}$, $\mathbf{S} \leftarrow \mathbf{0}_{N\times N}$, $\boldsymbol{\Upsilon} \leftarrow \mathbf{0}_{N\times K}$, $t \leftarrow 0$, $R_1 \leftarrow 0$, $R \leftarrow 0$, $P_s(\theta) \leftarrow 0$, $\hat{f} \leftarrow \mathbf{0}_{N-K}$, N, K_{max}, σ_{th}, σ_e, σ_w, ϵ, $|\psi\rangle$, L, κ
- **Output:** $P_s(\theta)$

1) **Step-1: Co-variance Matrix from Steering Arrays**
   For $n = 1 : L$, **do:**
   $\mathbf{s}(n) \leftarrow \boldsymbol{\Upsilon}^{\dagger}\mathbf{x}(n) + \boldsymbol{\eta}(n)$;
   $\mathbf{S} \leftarrow \mathbb{E}[\mathbf{s}\mathbf{s}^{\dagger}]$
   End For
2) **Step-2: Hamiltonian Simulation**
   for $j = 1 : m$, **do:**
   $t \leftarrow 1/m$;
   $U \leftarrow exp(-i\sum_j U_j t)$
   for $l = 1 : m$, **do:**
   $\tilde{U} \leftarrow \sum_{l=0}^{\kappa} \frac{1}{l!m^t}(-i\sum_j U_j)^l$
   while$(t > 0)$, **do:**
   If$(||U - \tilde{U}|| < \epsilon)$;
   break;
   End If
   End For
   End For
3) **Step-3: QPE**
   For $j = 1 : N$, **do:**
   $\phi_0 \leftarrow |0\rangle^{\otimes n} |\psi\rangle$;
   $\tilde{\psi}_1 \leftarrow \frac{1}{2^{n/2}}(|0\rangle + |1\rangle)^{\otimes n} |\psi\rangle$
   For $l = 1 : N$, **do:**
   $\tilde{\psi}_2 \leftarrow \frac{1}{2^{n/2}} \sum_{l=0}^{2^N-1} exp(2\pi i\theta_l) |l\rangle \otimes |\psi\rangle$
   For $l = 1 : N$, **do:**
   $\tilde{\psi}_3 \leftarrow \frac{1}{2^n} \sum_{h=0}^{2^N-1} \sum_{l=0}^{2^N-1} exp(\frac{2\pi ik}{2^N}(h - 2^n\theta)) |h\rangle \otimes |\psi\rangle$
   End For
   End For
   End For

Step-4: Spectrum Estimation

- **Sorting Eigenvalues**
  For $i = 1 : N$, **do:**
  $[\sigma, i] \leftarrow sort(\sigma_i)$
  End For
- **Spectrum Estimation:**
  If $K + 1 \leq N - K$, **do:**
  For $i = 1 : N - K$, **do:**
  $\hat{f} \leftarrow \frac{1}{\sum_{i=K+1}^{N} ||\mathbf{a}_i^{\dagger}(\theta)\psi_i||^2}$;
  $P_s(\theta) \leftarrow 10 \log_{10} (\hat{f})$
  End For
  End If

to classical MUSIC [43]. The estimated eigenvalues are sorted in classical registers. We can find K distinct eigenvectors corresponding to the highest K-eigenvalues as signal subspace, and the rest $N - K$ eigenvectors form the noise-subspace. As steering vectors lie on the signal subspace, which are orthogonal to the noise-subspace eigenvectors, we can find the spectral peaks using the expression given by

$$\hat{f} = \frac{1}{\sum_{i=K+1}^{N} ||\mathbf{a}_i^{\dagger}(\theta)\psi_i||^2}. \tag{41}$$

The locations of multiple sources can be estimated by searching the positions of the peaks in the spectrum function $P_s(\theta) = 10 \log_{10}(\hat{f})$ given by

$$\underset{\theta}{\arg\max} \; P_s(\theta). \tag{42}$$

Here, the scanning angle θ is taken to be $-\pi/2$ to $\pi/2$ radian, considering the angle of view of the sensors to be π radian. The computation of (42) can be performed using a line-search algorithm.

V. Analysis of Quantum Noise and Complexity on Proposed Algorithms

In this section, we discuss the measurement of uncertainty. Two kinds of errors are often encountered in quantum circuits. One is the gate-level error which includes shot noise, Markovian noise, the sensitivity of qubits due to flux-noise, quasi-particle tunnelling, qubit relaxation time, qubit de-phasing time (white noise) and others [44]. The other kind of error is the measurement error due to probabilistic quantum nature. In this work, we have considered that the circuit is ideal and gate-level errors are corrected [45] with at most ϵ error in the simulation. Here, we analyze the measurement error for the QEE problem we have discussed.

A. The Evolution Uncertainty

In preparation of the unitary operator $\mathbf{U}_N \in \mathbb{C}^{N\times N}$, we incur an error ϵ due to approximation of $\mathbf{U}_N$ through Hamiltonian simulation given by $||\mathbf{U}_N - e^{i\mathbf{S}t}||_2$. The perturbed evolution operator can be modelled as

$$\tilde{\mathbf{U}}_N = \mathbf{U}_N + \Delta\mathbf{U}_N, \tag{43}$$

where $\mathbf{U}_N$ is the unperturbed unitary matrix, and $\Delta\mathbf{U}_N$ denotes the perturbation component. We define the spectrum of $\mathbf{U}_N$ given by $\lambda(\mathbf{U}_N) = (\sigma_1, \sigma_2, \ldots, \sigma_N)$, and the spectrum of $\mathbf{U}_N + \Delta\mathbf{U}_N$ by $\lambda(\mathbf{U}_N + \Delta\mathbf{U}_N) = (\mu_1, \mu_2, \ldots, \mu_N)$. We can bound the estimation error in eigenvalues σ_i for $i = (1, \ldots, N)$ using Bauer-Fike theorem for 2-norm given as follows (Theorem 7.2.2 of [46])

$$\underset{\lambda\in\lambda(\mathbf{U}_N)}{min} ||\lambda_i - \mu_i|| \leq \kappa_2(\mathbf{X}) \; ||\Delta\mathbf{U}||_2 \tag{44}$$

where, $\lambda_i \in \lambda(\mathbf{U}_N)$, $\mu_i \in \lambda(\mathbf{U}_N + \Delta\mathbf{U}_N)$, and κ_2 is the condition number of $\mathbf{X}$ with $\mathbf{X}^{-1}\mathbf{U}_N\mathbf{X} = \boldsymbol{\Lambda} = \mathbf{diag}(\sigma_1, \sigma_2, \ldots, \sigma_N)$. Here, the matrix $\mathbf{X}$ is comprised of eigenvectors of the unitary matrix $\mathbf{U}_N$. As $\mathbf{U}_N$ is a normal matrix, its eigenvector matrix $\mathbf{X}$ is an orthonormal matrix (Theorem 2.5.3 of [47]). Hence, the value of $\kappa_2(\mathbf{X}) = ||\mathbf{X}||||\mathbf{X}^{-1}|| = 1$. Therefore, the mean square error of eigenvalue is bounded as $||\Delta\mathbf{U}||_2^2 \leq \epsilon^2$.

B. The Measurement Uncertainty

Let us consider that the experiment is repeated for $n = 1, \ldots, M$ times, with one or multiple rounds denoted by $r = 1, \ldots, R_n$. The ancilla qubit prepared in superposition state (with the application of Hadamard gate) controls $\mathcal{U}_c^{\tau_r}$ (13) with integer variable τ_r per round. With the application of the rotation gate, the ancilla qubit is read out in the X-basis and it returns a measurement outcome $m_r \in \{0, 1\}$. The total number of controlled-U rotation over M experiments is given by

$$\varrho_T = \sum_{n=1}^{M} \sum_{r=1}^{R_n} \tau_r, \tag{45}$$

Authorized licensed use limited to: ULAKBIM UASL - DOKUZ EYLUL UNIVERSITESI. Downloaded on October 28,2022 at 12:45:57 UTC from IEEE Xplore. Restrictions apply.

TABLE I
COMPUTATIONAL COMPLEXITY OF DIFFERENT QUANTUM SUB-ROUTINES

Sub-routine/Algorithm	Computational Complexity	Remark(Any)
Grover's search for $N \times 1$-unsorted array	$\mathcal{O}(\sqrt{N})$	$\mathcal{O}(N)$ for classical computers
N-tuple vector encoding	$\mathcal{O}(\sqrt{N})$	using amplitude amplification
N-tuple vector encoding	$\mathcal{O}(poly\ log(N))$	with augmented QRAM
Hamiltonian Simulation	$\mathcal{O}\left(\tau\log(\frac{\tau}{\epsilon})/\log\log(\frac{\tau}{\epsilon})\right)$	$\tau = d^2\|\|\mathbf{S}\|\|_{max}t \geq 1$ [28]
Quantum Phase Estimation (QPE)	$\mathcal{O}(\frac{1}{\epsilon}) \times \mathcal{O}\left(\tau\log(\frac{\tau}{\epsilon})/\log\log(\frac{\tau}{\epsilon})\right)$	U, H gates and $IQFT$.
QA-SDA	$\mathcal{O}(\frac{1}{\epsilon}) \times \mathcal{O}\left(\tau\log(\frac{\tau}{\epsilon})\log\log(\frac{\tau}{\epsilon})\right)$ + $\mathcal{O}(\sqrt{K_{max}})$	QPE, and oracle-comparison
QA-MUSIC	$\mathcal{O}(\frac{1}{\epsilon}) \times \mathcal{O}\left(\tau\log(\frac{\tau}{\epsilon})/\log\log(\frac{\tau}{\epsilon})\right)$ + $\mathcal{O}(\sqrt{N})$ + $\mathcal{O}(\sqrt{N-K})$	QPE, oracle-sorting, and AoA

and for each experiment the number of controlled-U rotation is $\varrho = \sum_{r=1}^{R_n} \tau_r$. The coherence length ϱ_{err} is defined in [45] as

$$\varrho_{err} = \frac{T_{err}}{N_q T_U}, \tag{46}$$

which limits the maximum number of applications of the controlled-U per experiment by $\varrho \leq \varrho_{err}$. Here, $\frac{T_{err}}{N_q}$ denotes time-to-failure of N_a qubits, T_U represents the time required to implement single controlled-U gate, and T_{err} is the time-to-error of a single qubit. Hence, the choice of ϱ is crucial and related to the QTR of the quantum hardware (qubits and registers in particular).

In a particular experiment, we consider that the controlled-rotation is $\mathcal{U}_c^{\tau_1}$ and the ancilla qubit is rotated by $\mathcal{R}_z(\beta_1) = \exp(-i\beta_1/2)$, where β_1 is the phase for rotation around the Z-axis direction. The outcome state generated from the eigenstate of the operator $\mathbf{U}$ is given by

$$\frac{1}{\sqrt{2}} \sum_j \alpha_j \left(|0\rangle + e^{i(\tau_1\sigma_j + \beta_1)}|1\rangle\right)|\psi_j\rangle, \tag{47}$$

where α_j is the normalizing coefficient for eigenstate $|\psi\rangle_j$ corresponding to eigenvalue σ_j. Due to repetition of the experiment, there is uncertainty in getting the outcome on a particular X-basis. The probability of measurement of the ancilla qubit on $m_r \in \{0, 1\}$ basis is given by

$$\sum_j B_j \cos^2\left(\frac{\tau_1\sigma_j}{2} + \frac{\beta_1 - m_r\pi}{2}\right), \tag{48}$$

where $B_j \equiv |\alpha_j|^2$. Hence, the outcome-state of the ancilla qubit becomes

$$\sum_j \tilde{\alpha}_j \exp\left(\frac{i}{2}\tau_1\sigma_j + \beta_r\right)\cos\left(\frac{\tau_1\sigma_j}{2} + \frac{\beta_r - m_r\pi}{2}\right)|\psi\rangle_j. \tag{49}$$

Here, $\tilde{\alpha}_j$'s are normalized coefficients for (49). Now, the probability of a bit's correct measurement outcome is given by

$$p_b = \frac{1}{N}\sum_{k=1}^{N}\sum_j B_j \prod_{r=1}^{R_n} \cos^2\left(\frac{\tau_r\sigma_k}{2} + \frac{\beta_r - m_r\pi}{2}\right), \tag{50}$$

where σ_k denotes the kth eigenvalue. We have already assumed that the quantum system has N_a-bits resolution and the probability of correctly measuring each single bit is determined as p_b in (50). Let x_i be the decimal value of ith binary string of length N_q. Let $x_{i,l}^k$ be a N_q length binary string with l bits reversed with respect to x_i and k indicates the kth realization of such string.

Proposition 1: The variance of the quantum measurement noise w_q for a N_q-bits quantum resolution system after the phase estimation is calculated as

$$\sigma_q^2 = K_q \sum_{i=1}^{2^{N_q}} \sum_{l=1}^{N_q} \sum_{k=1}^{{}^{N_q}C_l} p_b^l (1-p_b)^{N_q - l} \|x_i - x_{i,l}^k\|^2,$$
$$with\ K_q = \frac{1}{2^{N_q}\sum_{l=1}^{N_q} {}^{N_q}C_l \times N_q}. \tag{51}$$

Proof: The probability of l-bits mismatch for x_i is $p_b^l(1-p_b)^{N_q-l}$. It is assumed that the sign bit is equally prone to flip. Therefore, the mean of the error will be zero. There will be ${}^{N_q}C_l$ number of binary strings having l-bits in mismatch with respect to x_i and $l = 1, 2, \ldots, N_q$. The index i varies as $i = 1, 2, \ldots, 2^{N_q}$. Therefore, the average value of the error is calculated as in (51). ■

C. Analysis of Computational Complexity

The complexity class for the problems solved by a quantum computer using Quantum algorithms is commonly known as bounded-error quantum polynomial time (BQP). In our work, we take several quantum sub-routines which provide the exponential and quadratic speed-up as compared to classical algorithms for solving certain problems. We provide a list of different quantum subroutines and computational complexity in Table I. The key part here is the Hamiltonian simulation of the matrix $\mathbf{S}$ to prepare an optimal unitary operator $\mathbf{U}$. In our work, the Hamiltonian matrix, i.e, $\mathbf{S}$ is known in great detail. Additionally, the matrix is sparse in nature. Ideally, we expect the complexity of the quantum simulation to be $\mathcal{O}(||\mathbf{S}t||, \log N, \frac{1}{\epsilon})$, with the overall error in the simulation bounded by ϵ. For dense matrix $\mathbf{S}$, that is $d = N$ (where, d is sparsity and N is the dimension of $\mathbf{S}$), the computation does not provide a query complexity of $\mathcal{O}(||\mathbf{S}t||, \log N)$. However, as $\mathbf{S}$ is d-sparse with $d \ll N$, the unitary $\mathbf{U} = \mathbf{e^{-iSt}}$ can be efficiently simulated. The query complexity to such systems can be reduced to $\mathcal{O}(d + \log N)$ to an oracle for $\mathbf{S}$ [48]. This is a significant computation advantage for computing eigenvalues of $\mathbf{S}$ using QPE, as compared to classical EVD, where it is $\mathcal{O}(N^3)$ in general. For the sparse matrix scenario, where $K \ll N$, the complexity would be $\mathcal{O}(KN^2)$. For QA-SDA, in addition of QPE, we have the complexity of $\mathcal{O}(\sqrt{K_{max}})$ for quantum oracle based comparison for K_{max} sources. Similarly, in QA-MUSIC, we need a QRAM

Authorized licensed use limited to: ULAKBIM UASL - DOKUZ EYLUL UNIVERSITESI. Downloaded on October 28,2022 at 12:45:57 UTC from IEEE Xplore. Restrictions apply.

based sorting, as well as computing the phase of the signal (AOA), hence the overall complexity becomes $\mathcal{O}(\frac{1}{\epsilon}) \times \mathcal{O}\left(\tau \log(\frac{\tau}{\epsilon})/\log\log(\frac{\tau}{\epsilon})\right) + \mathcal{O}(\sqrt{N}) + \mathcal{O}(\sqrt{N-K})$. One can plug different array structure of $\mathbf{S}$, in addition to sparsity to check the complexity improvement of the quantum simulation, which remains an open area of research in quantum signal processing dealing with complexity issues.

D. Quantum Gate Complexity With Respect to Elementary Operations

For efficient implementation of the proposed semi-quantum algorithms (i.e, QA-SDA, and QA-MUSIC), we need quantum gates and QRAM memory. The central building block for the proposed algorithms is QPE. On successive estimation of the eigenvalues through QPE, one can store the eigenvalues on QRAM for further processing of the data as required for QA-SDA and QA-MUSIC respectively. The quantum gate complexity of the QPE is discussed as follows.

In a QPE circuit, we need multiple quantum gates and intermediate subroutine such as Hadamard gate, controlled-U rotation gate, and IQFT block (Ref. Chapter 5.2 of [32]). In addition, quantum registers are required for data encoding, processing and measurement. A quantum oracle is often required to prepare quantum states $|\psi\rangle_i$ (for $i = 1, 2, \ldots, N$) and perform controlled-U rotations as shown in (12).

- For a possible eigenstate $|\psi\rangle_i$ of the unitary operator $\mathbf{U}$, we can start with a first register comprising of b number of qubits $|0\rangle$ (which can be expressed as the power of 2) for a possible b-bits representation of the phase σ_i. To create superposition states of b-qubits, b number of Hadamard operations are required. A second register performs controlled-U^{2^j} rotations sequentially on the output of Hadamard gate, where j varies from 0 to $b-1$.
- Based on the output of the oracle after controlled-U rotations, an IQFT is performed which takes $C_1 = b(b+1)/2$ gates for Hadamard and rotations, and $C_2 = b/2$ swap-gate operations.
- The total number of elementary operations required is approximately $C_3 = 2b + C_1 + C_2 = 2b + b(b+1)/2 + b/2$. Hence, for N eigenvalue estimation, we need at least $C_4 = N \times C_3 = N \times (3b + b^2/2)$ operations approximately [32]. By increasing the ancillary qubits b in the first register, one can increase the precision of estimated value of σ_i on the measurement bases.
- Apart from the usual QPE operation, we need Hamiltonian simulation for unitary state preparation for the proposed QA-SDA and QA-MUSIC algorithms. Hence, we prepare unitary matrix $\mathbf{U}$ from the covariance matrix $\mathbf{S}$. It is performed by a method called Trotter-Suzuki approximation which enables us to express the exponential of sum of non-commuting operators ($e^{-i\sum_{j=1}^{n}\mathbf{S}_j t}$) in terms of product of unitary matrices. The gate complexity of the Hamiltonian simulation can be given as [49]

$$C_5 = \mathcal{O}\left(\frac{\tau \log^2(\frac{\tau}{\epsilon})}{\log\log(\frac{\tau}{\epsilon})}\right). \tag{52}$$

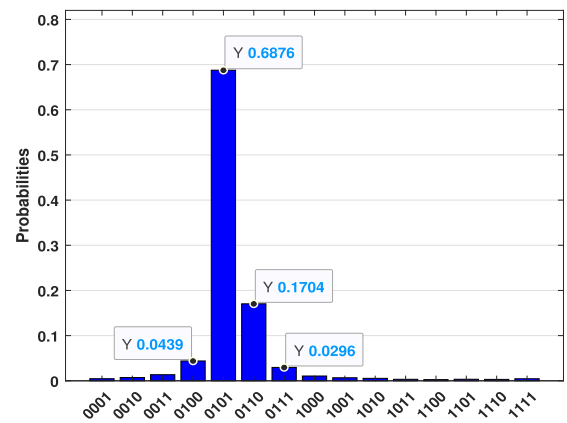

Fig. 3. Eigenvalues simulated on classical computer with Qiskit package with Hamiltonian simulation framework.

- Hence, the total gate complexity will be

$$\begin{aligned} C_{total} &= C_4 + C_5 \\ &= N \times (3b + b^2/2) + \mathcal{O}\left(\frac{\tau \log^2(\frac{\tau}{\epsilon})}{\log\log(\frac{\tau}{\epsilon})}\right). \end{aligned} \tag{53}$$

- However, for the classical matrix of dimension $N \times N$, the eigenvalue estimation complexity is $\mathcal{O}(N^3)$ [50].

VI. Numerical Results and Discussion

We consider a sensor array system having 10 sources with a different number of sensor antennas. We also demonstrate the quantum estimation of eigenvalues.

A. Eigenvalue Estimation With Hamiltonian Simulation for Sensor Array

We now show two different kinds of Hamiltonian simulation in this context, i.e sensor array data with 16 antennas: (i) Single quantum phase estimation and (ii) Multiple phase estimation. Some of the simulations are performed on IBM quantum simulators, and others on classical computer. Fig. 2 shows a circuit of QPE, where a shorter version has been simulated on IBM QISKIT quantum simulator [29] with four ancillary qubits represented by quantum registers q_0, q_1, q_2, and q_3. Single phase estimation is performed for the phase of first eigenvalue of $\mathbf{U}$, which provides the first eigenvalue of $\mathbf{S}$. Here, x contains the ith eigenstate ($|\psi\rangle_i$) stored in the quantum-register q_4, and c represents classical registers.

With 4-ancillary qubits, the experiment is evaluated for 10000 times to get the histogram of outcome probability of the phase on the measurement bases. A measurement basis is a binary string, whose length is controlled by the number of ancillary qubits. Fig. 3 shows the histogram of the measurement outcome of the simulation performed on a classical computer. Here, the optimal measurement basis for the measurement is 0101, which has the highest probability of occurrence ($p \approx 0.68$).

The same experiment is run on the IBM quantum simulator, as the histogram shown in Fig. 4. The vertical axis shows the probability of measurement, and the horizontal axis denotes

Authorized licensed use limited to: ULAKBIM UASL - DOKUZ EYLUL UNIVERSITESI. Downloaded on October 28,2022 at 12:45:57 UTC from IEEE Xplore. Restrictions apply.

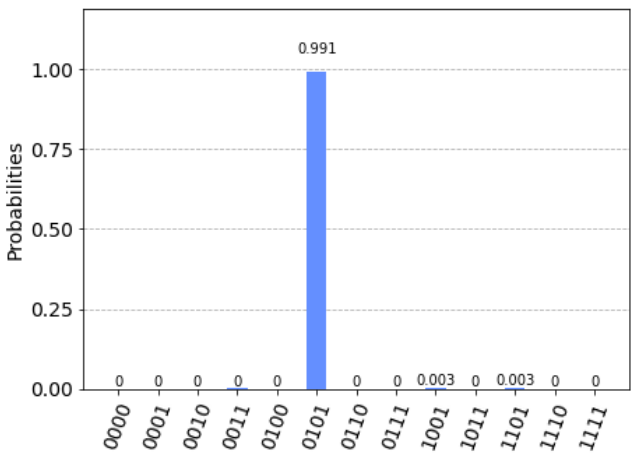

Fig. 4. Eigenvalues simulated on IBM quantum computer with Hamiltonian simulation framework.

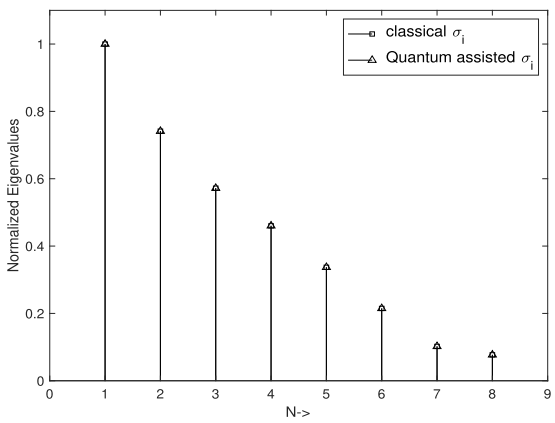

Fig. 5. Estimated Spectrum via EVD and QPE with optimal QTR.

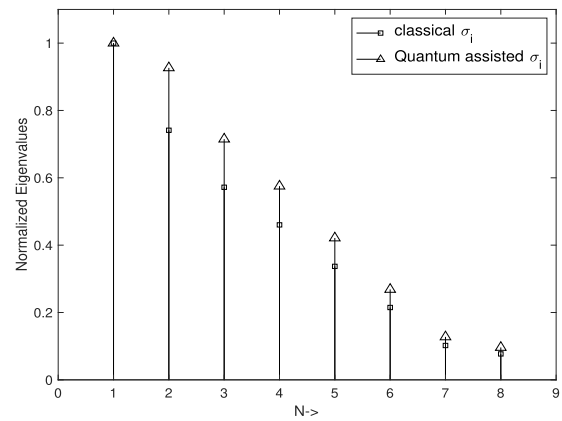

Fig. 6. Estimated Spectrum via EVD and QPE with sub-optimal QTR and measurement noise.

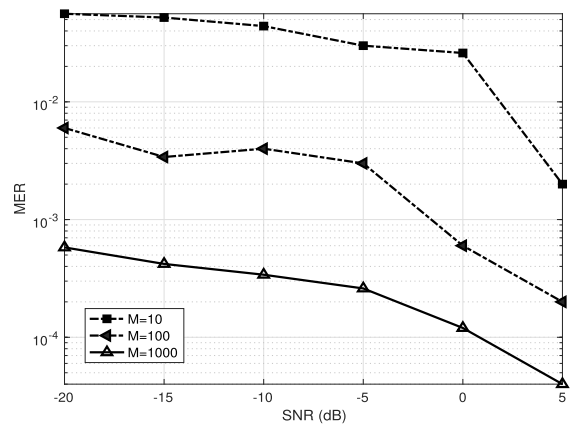

Fig. 7. Measurement error rate (MER) with SNR(dB) for different number of experiments (M).

the measurement bases. Here, other than the correct basis, all other bases are insignificant. The probability of occurrence of optimal basis is $p \approx 0.99$. The estimated phase via QPE is computed as

$$\hat{\sigma} = \frac{N_m}{2^{N_c}} \tag{54}$$

where, N_m is the decimal value of the binary string that represents the basis with the highest probability, and N_c is the number of ancillary qubits. With this setting, we have obtained the value of $\hat{\sigma}$ as 0.62, which is close to the true phase.

The difference in the eigenvalue estimation on a classical computer as shown in Fig. 3, and on a IBM quantum simulator (shown in Fig. 4) is due to the presence of noise in quantum measurement being significant in the classical computer.

Fig. 5 and Fig. 6 show the comparison between the eigenvalues estimated by EVD and QPE. We have shown that with a proper QTR of the covariance matrix $\mathbf{S}$, the estimated eigenvalues by EVD and QPE overlap as shown in Fig. 5. For the covariance matrix simulation, the QTR is taken to be 0.0056.

In Fig. 6, we have shown the eigenvalues estimated by QPE and EVD. Here, the estimated eigenvalues by QPE is degraded as compared to the standard EVD (considering QPE has measurement uncertainty with zero mean, and standard deviation of 0.2 for Gaussian probability density function). Finally, we define the quality of service (QoS) parameter called measurement error rate (MER) as follows

$$MER = \frac{N_{E_s}}{N_{T_s}}, \tag{55}$$

where, N_{E_s} is the number of bases that wrongly represent the measurement outcome, and N_{T_s} is the total number of measurement basis. Here, the signal to noise ratio (SNR) arises because the measurement noise creates uncertainty in detecting the signal, which is binary strings here. Considering the string length of $M = 10, 100, 1000$ with Gaussian noise as a special case, we have shown the MER versus SNR plot in Fig. 7. It is shown that with a larger string length, the MER decays exponentially.

B. Detection Performance With QEE

In Fig. 8, the QA-MUSIC spectrum for 10-signal sources are shown. The actual positions are shown as square boxes horizontally, whereas the estimated AoAs are represented by the locations of peaks of the spectrum function, $\mathbf{P}_s(\theta)$. Here, the sources are assumed to be distributed uniformly within $-\pi/2$ to $\pi/2$ radian. The array size is considered to be 128, which provides the sparsity in $\mathbf{S}$ as $N \gg K$. The simulation is

Authorized licensed use limited to: ULAKBIM UASL - DOKUZ EYLUL UNIVERSITESI. Downloaded on October 28,2022 at 12:45:57 UTC from IEEE Xplore. Restrictions apply.

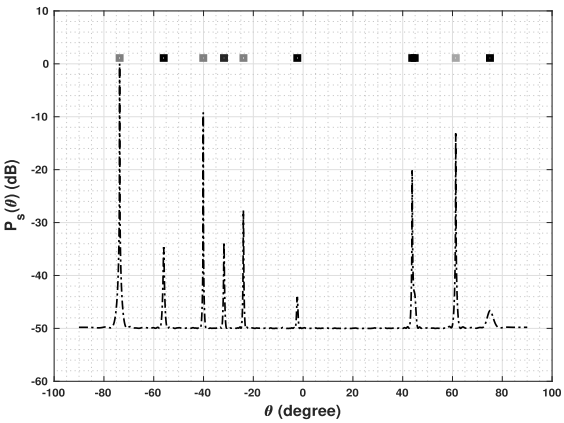

Fig. 8. QA-MUSIC: Estimated angles for 10 sources (uniformly distributed in $-\pi/2$ to $\pi/2$) and 128 arrays.

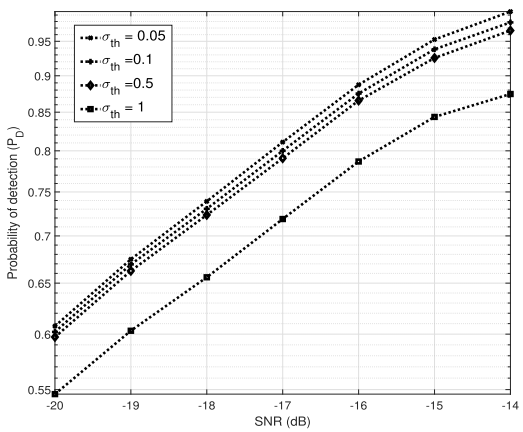

Fig. 9. QA-SDA: Probability of detection (P_D) with SNR (dB) at different detection threshold.

performed keeping a lower noise variance. The SNR is chosen as 18 dB with signal power being 0.5 watt. It is observed that the QA-MUSIC determines the location of the sources almost accurately. In Fig. 9, we have shown the probability of detection (P_D) with SNR (in dB), at different detection threshold, $\sigma_{th} = 0.01, 0.1, 0.5, 1$ respectively, using QA-SDA simulation. Here, the actual number of sources is 10, and different curves represent the performance of the detector for different σ_{th}.

Fig. 10 represents the optimal values of detection threshold vs. the SNR for different probability of detection (0.95, 0.85) as obtained from (40). With higher SNR values, the optimal σ_{th} is reduced. This is because as the the noise reduces, detection threshold needs to be reduced to detect smaller eigenvalues. This trend has been confirmed from (9). Another observation at the lower SNR is that if the lower probability of detection is intended, the σ_{th} needs lower values as the noise level is already high. However, at the higher SNR, σ_{th} needs to be larger to meet the lower probability of detection requirement.

C. Discussion on Quantum Advantages for Large Sensor Arrays

The proposed algorithms QA-SDA and QA-MUSIC via QEE framework as shown in our work is expected to provide

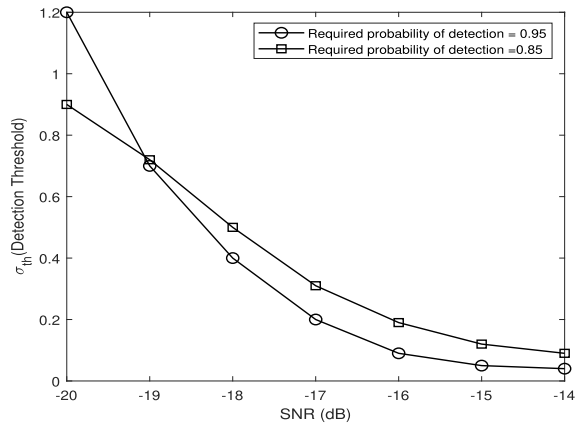

Fig. 10. Proposed Detection Threshold (σ_{th}): This is the plot of σ_{th} (detection threshold) variation with respect to SNR for multiple probability of detection as obtained from (40).

complexity advantages for some upcoming large sensor array applications in signal processing and communications. Here, the numerical simulation framework considers a practical array application where signals are captured from a few objects incident on a large antenna arrays to demonstrate the applicability of the proposed algorithms. Further, the large array can be a few hundreds in size for a base-station in massive MIMO-communication system [51], and it can be even as large as 1024×1024 for a plasmonic nano sensor in ultra-massive multiple-input multiple-output (UM MIMO) THz communications [52]. The proposed framework is expected to have potential complexity-advantage in such similar large sensor array applications.

VII. Conclusion

In this article, we have shown a Hamiltonian simulation-based quantum framework for the detection and estimation of signal parameters via quantum phase estimation. The quantum assisted algorithms provide significant complexity reduction in computing eigenvalues of a sparse-Hamiltonian system matrix obtained from the sensor array model. A systematic approach of quantum assisted simulation of the Hamiltonian is shown with a small-scale implementation on the IBM quantum simulator, while large-scale implementation is performed on a classical system. The maximization of the measurement outcome probability is obtained by Bayesian inference, keeping an error model inside to incorporate QTR from different circuits. Further, we have defined a QoS parameter to showcase the measurement error rate (MER) at different noise level and repetition of the experiment. The context of QTR is considered while comparing EVD and QPE. We have shown the computational complexity of the given framework for possible applications in array-processing.

References

[1] S. Payami, M. Ghoraishi, and M. Dianati, "Hybrid beamforming for large antenna arrays with phase shifter selection," *IEEE Trans. Wireless Commun.*, vol. 15, no. 11, pp. 7258–7271, Nov. 2016.

[2] X. Gao, L. Dai, Y. Zhang, T. Xie, X. Dai, and Z. Wang, "Fast channel tracking for terahertz beamspace massive MIMO systems," *IEEE Trans. Veh. Technol.*, vol. 66, no. 7, pp. 5689–5696, Jul. 2017.

Authorized licensed use limited to: ULAKBIM UASL - DOKUZ EYLUL UNIVERSITESI. Downloaded on October 28,2022 at 12:45:57 UTC from IEEE Xplore. Restrictions apply.

[3] C. Lin and G. Y. Li, "Indoor terahertz communications: How many antenna arrays are needed?" *IEEE Trans. Wireless Commun.*, vol. 14, no. 6, pp. 3097–3107, Jun. 2015.

[4] B. Peng, K. Guan, A. Kuter, S. Rey, M. Patzold, and T. Kuerner, "Channel modeling and system concepts for future terahertz communications: Getting ready for advances beyond 5G," *IEEE Veh. Technol. Mag.*, vol. 15, no. 2, pp. 136–143, Jun. 2020.

[5] H. Zhao, N. Zhang, and Y. Shen, "Beamspace direct localization for large-scale antenna array systems," *IEEE Trans. Signal Process.*, vol. 68, pp. 3529–3544, 2020.

[6] P. Chen, Z. Cao, Z. Chen, and X. Wang, "Off-grid DOA estimation using sparse Bayesian learning in MIMO radar with unknown mutual coupling," *IEEE Trans. Signal Process.*, vol. 67, no. 1, pp. 208–220, Jan. 2018.

[7] W. T. Vetterling *et al.*, *Numerical Recipes: Example Book C*. Cambridge, U.K.: Cambridge Univ. Press, 1992.

[8] E. Tang, "A quantum-inspired classical algorithm for recommendation systems," in *Proc. 51st Annu. ACM SIGACT Symp. Theory Comput.*, Jun. 2019, pp. 217–228.

[9] L. Hanzo, H. Haas, S. Imre, D. O'Brien, M. Rupp, and L. Gyongyosi, "Wireless myths, realities, and futures: From 3G/4G to optical and quantum wireless," *Proc. IEEE*, vol. 100, pp. 1853–1888, May 2012.

[10] S. X. Ng *et al.*, "Guest editorial advances in quantum communications, computing, cryptography, and sensing," *IEEE J. Sel. Areas Commun.*, vol. 38, no. 3, pp. 405–412, Mar. 2020.

[11] R. Cane, D. Chandra, S. X. Ng, and L. Hanzo, "Mitigation of decoherence-induced quantum-bit errors and quantum-gate errors using Steane's code," *IEEE Access*, vol. 8, pp. 83693–83709, 2020.

[12] L. K. Grover, "A fast quantum mechanical algorithm for database search," in *Proc. Annu. ACM Symp. Comput. (STOC)*, May 1996, pp. 212–219.

[13] C. Durr and P. Hoyer, "A quantum algorithm for finding the minimum," 1996, *arXiv:quant-ph/9607014*.

[14] D. W. Berry, G. Ahokas, R. Cleve, and B. C. Sanders, "Efficient quantum algorithms for simulating sparse Hamiltonians," *Commun. Math. Phys.*, vol. 270, no. 2, pp. 359–371, 2007.

[15] Y. Nam, Y. Su, and D. Maslov, "Approximate quantum Fourier transform with *O(n log(n))* T gates," *NPJ Quantum Inf.*, vol. 6, no. 1, pp. 1–6, Dec. 2020.

[16] P. Botsinis, D. Alanis, Z. Babar, S. X. Ng, and L. Hanzo, "Iterative quantum-assisted multi-user detection for multi-carrier interleave division multiple access systems," *IEEE Trans. Commun.*, vol. 63, no. 10, pp. 3713–3727, Oct. 2015.

[17] P. Botsinis *et al.*, "Quantum-assisted indoor localization for uplink mm-wave and downlink visible light communication systems," *IEEE Access*, vol. 5, pp. 23327–23351, 2017.

[18] P. Botsinis, D. Alanis, Z. Babar, S. X. Ng, and L. Hanzo, "Noncoherent quantum multiple symbol differential detection for wireless systems," *IEEE Access*, vol. 3, pp. 569–598, 2015.

[19] P. Botsinis, S. X. Ng, and L. Hanzo, "Low-complexity iterative quantum multi-user detection in SDMA systems," in *Proc. IEEE Int. Conf. Commun. (ICC)*, Jun. 2014, pp. 5592–5597.

[20] P. Botsinis, D. Alanis, Z. Babar, S. X. Ng, and L. Hanzo, "Joint quantum-assisted channel estimation and data detection," *IEEE Access*, vol. 4, pp. 7658–7681, 2016.

[21] P. Botsinis *et al.*, "Quantum-aided multi-user transmission in non-orthogonal multiple access systems," *IEEE Access*, vol. 4, pp. 7402–7424, 2016.

[22] W. Ye, W. Chen, X. Guo, C. Sun, and L. Hanzo, "Quantum search-aided multi-user detection for sparse code multiple access," *IEEE Access*, vol. 7, pp. 52804–52817, 2019.

[23] C. Wei, X. Zhou, L. Wang, P. Tian, and L. Hanzo, "Soft iterative quantum receivers approaching the Helstrom limit using realistic quantum devices," *IEEE Access*, vol. 6, pp. 10197–10207, 2018.

[24] D. Alanis *et al.*, "A quantum-search-aided dynamic programming framework for Pareto optimal routing in wireless multihop networks," *IEEE Trans. Commun.*, vol. 66, no. 8, pp. 3485–3500, Aug. 2018.

[25] S. Mondal, M. R. Laskar, and A. K. Dutta, "ML criterion based signal detection of a MIMO-OFDM system using quantum and semi-quantum assisted modified DHA/BBHT search algorithm," *IEEE Trans. Veh. Technol.*, vol. 70, no. 2, pp. 1688–1698, Feb. 2021.

[26] N.-H. Chia, H.-H. Lin, and C. Wang, "Quantum-inspired sublinear classical algorithms for solving low-rank linear systems," 2018, *arXiv:1811.04852*.

[27] D. Jethwani, F. L. Gall, and S. K. Singh, "Quantum-inspired classical algorithms for singular value transformation," 2019, *arXiv:1910.05699*.

[28] D. W. Berry, A. M. Childs, R. Cleve, R. Kothari, and R. D. Somma, "Exponential improvement in precision for simulating sparse Hamiltonians," in *Proc. 46th Annu. ACM Symp. Comput.*, May 2014, pp. 283–292.

[29] H. Abraham *et al.*, "Qiskit: An open-source framework for quantum computing," IBM, New York, NY, USA, Tech. Rep., 2019, doi: 10.5281/zenodo.2562111.

[30] R. Couillet and M. Debbah, *Random Matrix Methods for Wireless Communications*. Cambridge, U.K.: Cambridge Univ. Press, 2011.

[31] H. Li, P. Stoica, and J. Li, "Computationally efficient maximum likelihood estimation of structured covariance matrices," *IEEE Trans. Signal Process.*, vol. 47, no. 5, pp. 1314–1323, May 1999.

[32] M. A. Nielsen and I. Chuang, "Quantum computation and quantum information," MTI, Cambridge Univ. Press Edinburgh Building, Cambridge, U.K., Tech. Rep., 2002 doi: 10.1119/1.1463744.

[33] D. W. Berry, A. M. Childs, R. Cleve, R. Kothari, and R. D. Somma, "Simulating Hamiltonian dynamics with a truncated Taylor series," *Phys. Rev. Lett.*, vol. 114, no. 9, Mar. 2015, Art. no. 090502.

[34] G. H. Low and I. L. Chuang, "Hamiltonian simulation by qubitization," *Quantum*, vol. 3, p. 163, Jul. 2019.

[35] D. W. Berry, A. M. Childs, and R. Kothari, "Hamiltonian simulation with nearly optimal dependence on all parameters," in *Proc. IEEE 56th Annu. Symp. Found. Comput. Sci.*, Oct. 2015, pp. 792–809.

[36] A. Patel, "Optimisation of quantum evolution algorithms," 2015, *arXiv:1503.01429*.

[37] G. M. D'Ariano, C. Macchiavello, and M. F. Sacchi, "On the general problem of quantum phase estimation," *Phys. Lett. A*, vol. 248, nos. 2–4, pp. 103–108, Nov. 1998.

[38] F. Chapeau-Blondeau and E. Belin, "Fourier-transform quantum phase estimation with quantum phase noise," *Signal Process.*, vol. 170, May 2020, Art. no. 107441.

[39] M. Guo, Y. D. Zhang, and T. Chen, "DOA estimation using compressed sparse array," *IEEE Trans. Signal Process.*, vol. 66, no. 15, pp. 4133–4146, Aug. 2018.

[40] S. A. Hamza and M. G. Amin, "Hybrid sparse array beamforming design for general rank signal models," *IEEE Trans. Signal Process.*, vol. 67, no. 24, pp. 6215–6226, Dec. 2019.

[41] J. Grouffaud, P. Larzabal, and H. Clergeot, "Some properties of ordered eigenvalues of a Wishart matrix: Application in detection test and model order selection," in *Proc. IEEE Int. Conf. Acoust., Speech, Signal Process. Conf.*, vol. 5, May 1996, pp. 2463–2466.

[42] P. Stoica *et al.*, "Spectral analysis of signals," Prentice hall, Upper Saddle River, New Jersey, USA, Tech. Rep., 2005.

[43] R. O. Schmidt, "Multiple emitter location and signal parameter estimation," *IEEE Trans. Antennas Propag.*, vol. AP-34, no. 3, pp. 276–280, Mar. 1986.

[44] T. E. O'Brien, B. Tarasinski, and L. DiCarlo, "Density-matrix simulation of small surface codes under current and projected experimental noise," *NPJ Quantum Inf.*, vol. 3, no. 1, pp. 1–8, Dec. 2017.

[45] T. E. O'Brien, B. Tarasinski, and B. M. Terhal, "Quantum phase estimation of multiple eigenvalues for small-scale (noisy) experiments," *New J. Phys.*, vol. 21, no. 2, Feb. 2019, Art. no. 023022.

[46] G. H. Golub and C. F. Van Loan, *Matrix Computations*, 3rd ed. North Charles Street, Baltimore, MD, Johns Hopkins Univ. Press, 1996.

[47] R. A. Horn and C. R. Johnson, *Matrix Analysis*. Cambridge, U.K.: Cambridge Univ. Press, 2012.

[48] A. M. Childs and R. Kothari, "Simulating sparse Hamiltonians with star decompositions," in *Proc. Conf. Quantum Comput., Commun., Cryptogr.* Berlin, Germany: Springer, 2010, pp. 94–103.

[49] A. M. Childs, D. Maslov, Y. Nam, N. J. Ross, and Y. Su, "Toward the first quantum simulation with quantum speedup," *Proc. Nat. Acad. Sci. USA*, vol. 115, no. 38, pp. 9456–9461, 2018.

[50] V. Y. Pan and Z. Q. Chen, "The complexity of the matrix eigenproblem," in *Proc. 31st Annu. ACM Symp. Comput. (STOC)*, 1999, pp. 507–516.

[51] J. Du, M. Han, Y. Chen, L. Jin, and F. Gao, "Tensor-based joint channel estimation and symbol detection for time-varying mmWave massive MIMO systems," *IEEE Trans. Signal Process.*, vol. 69, pp. 6251–6266, 2021.

[52] I. F. Akyildiz, A. Kak, and S. Nie, "6G and beyond: The future of wireless communications systems," *IEEE Access*, vol. 8, pp. 133995–134030, 2020.

Authorized licensed use limited to: ULAKBIM UASL - DOKUZ EYLUL UNIVERSITESI. Downloaded on October 28,2022 at 12:45:57 UTC from IEEE Xplore. Restrictions apply.